Equation-of-state data for CsCl-type alkali halides

1997 J. Phys.: Condens. Matter 9 5581

(http://iopscience.iop.org/0953-8984/9/26/007)

J. Phys.: Condens. Matter **9** (1997) 5581–5592. Printed in the UK PII: S0953-8984(97)79737-6

Equation-of-state data for CsCl-type alkali halides

U Köhler, P G Johannsen and W B Holzapfel
Fachbereich Physik, Universität GH Paderborn, D-33095 Paderborn, Germany

Received 21 November 1996, in final form 10 March 1997

Abstract. Energy-dispersive x-ray diffraction (EDXD), with synchrotron radiation and diamond anvil cells (DAC), is used with different pressure sensors to determine the lattice parameters and equations of state (EOS) at room temperature, and pressures up to typically 40 GPa, for KBr, KI, RbCl, RbBr, RbI, CsCl, and CsBr. A comparison with previous literature data obtained by various techniques, and for different ranges of pressure indicates that all of the data fit to a recently proposed 'simple' first-order EOS form.

1. Introduction

For the discussion of recent accurate measurements of the refractive index for most of the alkali halides under pressure [1], as well as for the use of alkali halides as reference materials in pressure determinations with high-pressure x-ray diffraction, it appeared necessary to redetermine the pressure–volume relation at ambient temperature of several alkali halides, especially in those cases in which a phase transition from the low-pressure NaCl-type structure ($cF8$) to the CsCl-type structure ($cP2$) occurs at moderate pressures [2]. Thereby the following questions needed some special attention.

(1) What is the absolute uncertainty in the equation-of-state (EOS) data determined by means of different techniques, and especially by energy-dispersive x-ray diffraction (EDXD) using different high-pressure sensors [3]?

(2) Are there any significant differences between ultrasonic determinations of the values for the isothermal bulk modulus K_0 and its pressure derivative K_0' at ambient pressure with respect to the corresponding values derived from volumetric or EDXD measurements under pressure?

(3) Can one represent the EOS data for the alkali halides by 'simple' EOS forms, and what are the corresponding parameter values for the high-pressure phases to be used in the evaluation of other high-pressure data [4]?

2. The H11 equation of state

Various mathematical forms have been proposed for the representation of experimental pressure–volume data [5, 6]. These functions usually contain the parameters V_0, K_0, K_0', K_0'', ..., i.e. the ambient pressure values for the volume, the isothermal bulk modulus, and its pressure derivatives. If the substance under consideration does not undergo a phase transition in the experimental pressure range, the parameter V_0 is generally known with sufficient accuracy, and also K_0 may be accurately known from ultrasonic measurements. In these cases, only the pressure derivatives of the bulk modulus are free parameters.

0953-8984/97/265581+12$19.50

For the description of a high-pressure phase, on the other hand, the volume at ambient pressure is generally known only for the other crystal structure, and is thus not a 'good' parameter for use in an EOS function. The same applies, of course, to the bulk modulus for ambient conditions. Thus, at least three fitting parameters appear to be necessary for the representation of ambient temperature EOS data for such a high-pressure phase.

Typical experimental set-ups for the determination of EOS data consist of a gasketed DAC for the pressure generation using the ruby-luminescence technique for pressure measurements, and x-ray diffraction for the determination of the lattice parameters. Thereby typical uncertainties in pressure determinations are of the order of 5–10% [3], which means that the three parameters needed for determining the EOS of a high-pressure phase are generally not well determined by the experimental data. Systematic trends in a class of materials, like the alkali halides in the present case, may be obscured by the statistical scatter of the data. Thus, a reduction of the number of free parameters, as well as a reduction of the pressure uncertainty are needed, especially for the high-pressure phases.

In the H11-EOS form [6]

$$p = 3K_0 \frac{1-X}{X^5} \exp\left[c_0(1-X)\right] \tag{1}$$

with

$$X = (V/V_0)^{1/3} \tag{2}$$

the parameter c_0 is related to the first pressure derivative of the bulk modulus:

$$c_0 = \frac{3}{2}(K_0' - 3) \tag{3}$$

and through the form

$$c_0 = -\ln(3K_0/p_{FG0}) \tag{4}$$

and also to the pressure of a Fermi gas with

$$p_{FG0} = a_{FG}(Z/V_0)^{5/3} \tag{5}$$

where Z is the number of electrons in the volume V_0, and the universal constant a_{FG} has the value

$$a_{FG} = 23.369 \text{ MPa nm}^5. \tag{6}$$

Thus, if a class of substances shows the simple behaviour described by this H11-EOS, a reduction of free EOS parameters can be achieved, as K_0' can be calculated from Z, V_0, and K_0 by means of equations (3)–(6). In the next section, the available literature data for K_0' for the alkali halides will be compared to the predictions of the H11 form, to support the use of this form also for high-pressure phases, where data for V_0 and K_0 are usually not available.

3. K_0' systematics of the alkali halides

Ultrasonic values of K_0' for the lithium, sodium, potassium, and rubidium halides, which exhibit the $cF8$-structure at ambient conditions, have been compiled in a series of articles [7]. These data are given in the fourth column of table 1 together with the respective values for the three caesium halides, which crystallize in the $cP2$-structure [8]. With the use of a Born model [9, 10], the values for the repulsive potential parameters can be derived from the knowledge of V_0 and K_0 [7], and the respective Born parameters determine the corresponding values for K_0', given in the fifth column of table 1. The sixth column contains

Table 1. A comparison of values for K_0', derived from ultrasonic measurements (a) [7, 8], from Born model calculations (b) [7], and from the H11 linearization scheme (c) (using the literature values for V_0 [11, 27] and K_0 [7, 8] given also in this table).

Substance	V_0 (cm^3 mol^{-1})	K_0 (GPa)	K_0' (a)	(b)	(c)
LiF ($cF8$)	9.82	66.51	5.30	4.02	4.30
LiCl ($cF8$)	20.42	29.68	5.63	4.52	4.59
LiBr ($cF8$)	25.02	23.52	5.68	4.70	5.23
LiI ($cF8$)	33.17	17.26	6.15	4.93	5.56
NaF ($cF8$)	14.98	46.48	5.25	4.46	4.64
NaCl ($cF8$)	27.01	23.68	5.38	4.82	4.81
NaBr ($cF8$)	32.16	19.47	5.44	4.99	5.29
NaI ($cF8$)	40.81	14.87	5.58	5.19	5.58
KF ($cF8$)	23.00	30.22	5.38	4.88	4.82
KCl ($cF8$)	37.50	17.35	5.46	5.21	4.93
KBr ($cF8$)	43.28	14.64	5.47	5.26	5.33
KI ($cF8$)	53.11	11.51	5.56	5.39	5.58
RbF ($cF8$)	27.18	26.68	5.69	5.17	5.27
RbCl ($cF8$)	43.20	15.58	5.62	5.45	5.29
RbBr ($cF8$)	49.37	13.24	5.59	5.54	5.57
RbI ($cF8$)	59.78	10.49	5.60	5.69	5.76
CsCl ($cP2$)	42.18	16.74	5.98		5.58
CsBr ($cP2$)	47.73	14.34	5.95		5.80
CsI ($cP2$)	57.40	11.89	5.93		5.93

the values for K_0' corresponding to the H11 form (equations (2)–(5)). The values for V_0 [11] and K_0 [7], used in this evaluation, are given in the second and third column.

The following trends can be noticed in table 1: the K_0'-values obtained from the two semi-empirical models are remarkably close, while the experimental data appear to be systematically larger. However, for the substances of the present paper, i.e. for the chlorides, bromides, and iodides of potassium, rubidium, and caesium, the differences between the three respective values are rather small with respect to the typical experimental uncertainty. From these observations, it can be concluded that the H11 form represents very well the existing EOS data for the heavier alkali halides, which lends some confidence in the use of this form also for the representation of the data for the high-pressure phases with only two free parameters, namely V_0 and K_0. The deviations between the ultrasonic and theoretical values of K_0' for the lighter alkali halides will be discussed in a forthcoming paper [12].

4. Experimental details

Diamond anvil cells (DAC) [13, 14] with Inconel X 650 gaskets, and typical diameters of the central holes in these gaskets of 200 μm were usually used. The samples [15] were either mixed with one of the x-ray 'marker' materials NaCl, Au, or Cu [16–18], or embedded in a pressure-transmitting fluid [19], together with a ruby splinter of typically 10 μm diameter for pressure measurements by the ruby-luminescence technique [20] using the nonlinear ruby scale [17].

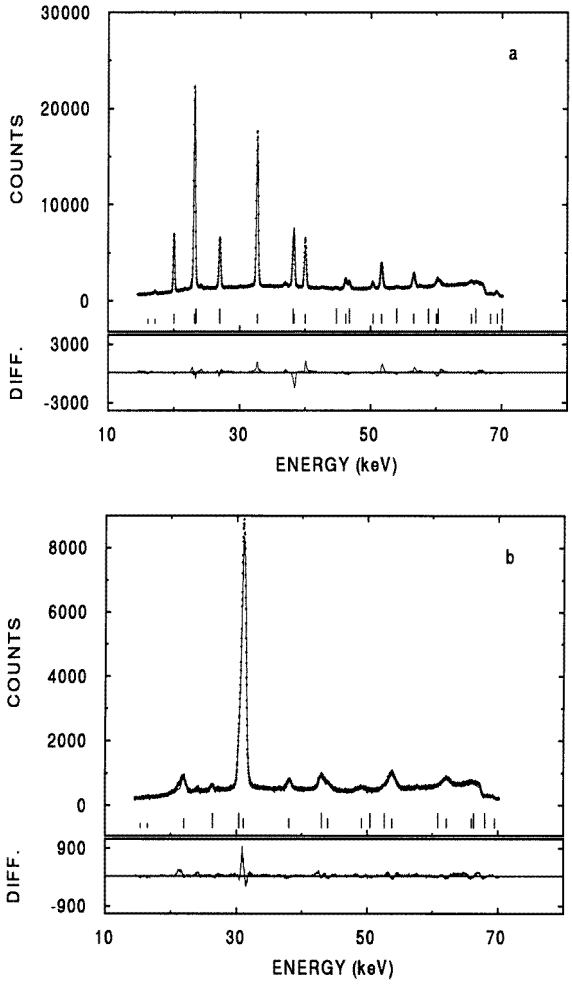

Figure 1. A typical EDXD spectrum for KBr with the pressure marker NaCl at ambient pressure (a) and 20.5 GPa (b). The diffraction angle was $2\delta = 9.350^{\circ}$. Points represent measured data, continuous lines give the fitted curves, and vertical lines show peak positions: short lines represent escape and fluorescence lines, medium lines represent sample Bragg peaks, and long lines represent pressure marker reflections.

The x-ray measurements on these polycrystalline samples in the DAC were performed in the energy-dispersive mode (EDXD), with synchrotron radiation, in HASYLAB, DESY, as described previously [21, 22]. The lattice parameters were fitted using a new program 'ProfFit', currently under development by one of the authors (UK). Typical spectra at ambient and higher pressures for KBr samples, with either NaCl or Au as the pressure marker, are shown in figure 1 and figure 2, respectively, where the measured data are represented by dots, and the fitted curves by continuous lines. For the fits of the theoretical curves to the data, the following parameters were used in the refinement.

(1) The (cubic) lattice parameters of the sample and the marker, to refine Gauss peaks (produced by the detector) at the line positions indicated in figures 1 and 2 by shorter and longer vertical lines below the spectra.

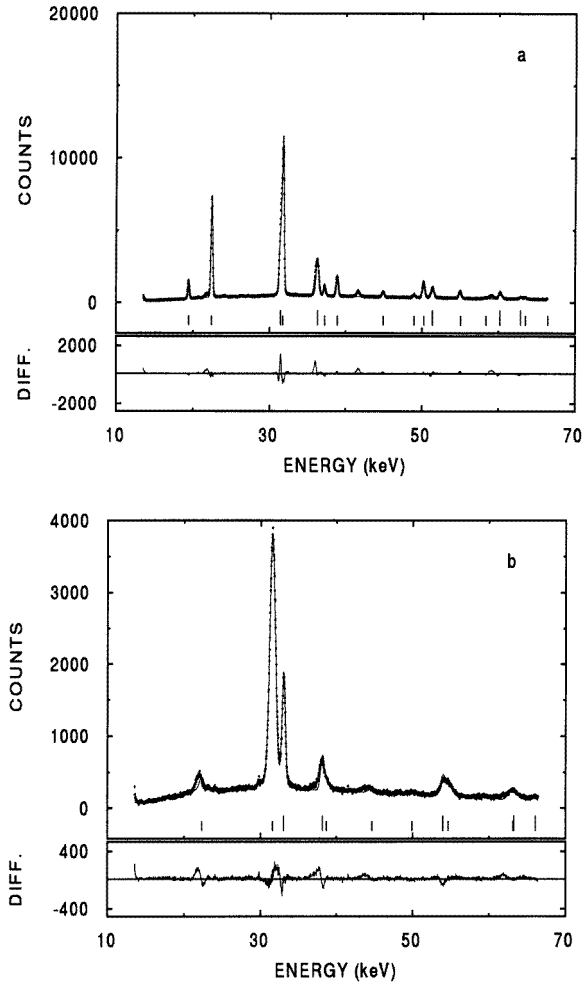

Figure 2. A typical EDXD spectrum for KBr with the pressure marker Au at ambient pressure (a) and 38 GPa (b). The diffraction angle was $2\delta = 9.606^\circ$. Points represent measured data, continuous lines give the fitted curves, and vertical lines show peak positions: short lines represent escape and fluorescence lines, medium lines represent sample Bragg peaks, and long lines represent pressure marker reflections.

(2) Pressure broadenings of the linewidths, and their energy dependence are approximated by a linear term with two extra parameters for each substance.

(3) One intensity parameter was used for each line.

(4) A set of 20 parameters was used to model the background by a spline.

(5) Additional parameters were used to fit the intensities of the x-ray fluorescence lines in the spectra of compounds with Rb, Cs, Br, and I.

(6) Additional intensity parameters were also used to model the weak escape lines produced by the detector at lower energies.

The differences between the measured data and fitted curves are illustrated below the spectra by the 'DIFF.' curves. Typically, the statistical uncertainty in the lattice parameter determination by this procedure is smaller than 0.05 pm for a spectrum with six or more

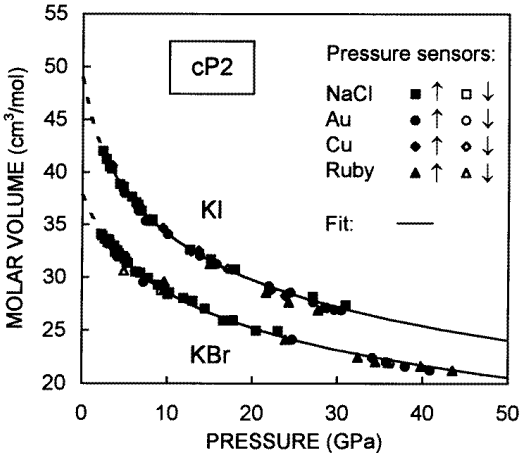

Figure 3. The pressure–volume relation of KBr and KI. Different symbols denote experiments with different pressure sensors. Full symbols stand for data points obtained after the increase of the pressure (↑), and open symbols for data points obtained after the decrease of the pressure (↓). The solid line represents the H11 form. The dashed line illustrates the extrapolation of the H11 form to ambient pressure in the region of the $cF8$-phase.

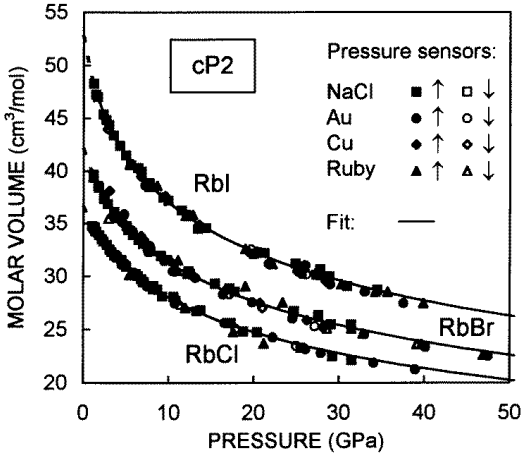

Figure 4. The pressure–volume relation of RbCl, RbBr, and RbI. Different symbols denote experiments with different pressure sensors. Full symbols stand for data points obtained after the increase of the pressure (↑), and open symbols for data points obtained after the decrease of the pressure. The solid line represents the H11 form. The dashed line illustrates the extrapolation of the H11 form to ambient pressure in the region of the $cF8$-phase.

well resolved lines for each substance (see, e.g., figure 2(a)). One error in the determination of the (cubic) lattice parameters and corresponding unit-cell volumes in the present study can be traced back to nonhydrostatic conditions, which induce deviatoric stresses [23, 24] and pressure gradients in the sample space. These effects can be noticed with the present procedures either as large s-shaped deviations in the 'DIFF.' curves or as special additional broadenings of the lines, as illustrated for instance in figure 2(b). A complete evaluation of the corresponding Singh–Kennedy effect could not be performed in the present study,

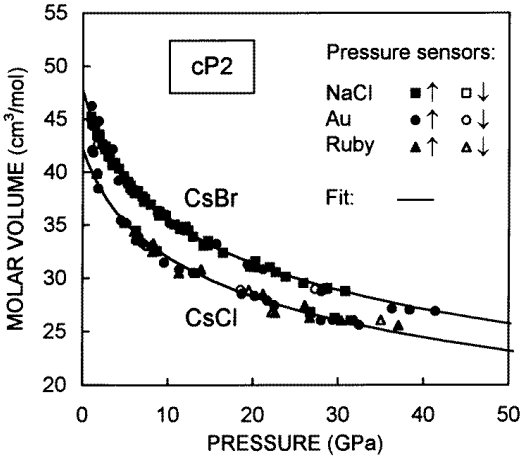

Figure 5. The pressure–volume relation of CsCl and CsBr. Different symbols denote experiments with different pressure sensors. Full symbols stand for data points obtained after the increase of the pressure (↑), and open symbols for data points obtained after the decrease of the pressure (↓). The solid line represents the H11 form. The dashed line illustrates the extrapolation of the H11 form to ambient pressure in the region of the $cF8$-phase.

Table 2. Parameters for the fitted form H11. For KCl, for which measurements have not been made in the present work, literature data [25, 26] have been used to obtain 'best values' of V_0, K_0, and K_0' for comparison (superscript a). For the caesium halides, the known values for V_0 at ambient conditions [27] have been used as pre-fixed values (superscript b). The literature values for K_0 and K_0' of CsI [8] are shown for comparison (superscript c). The numbers in brackets represent only the statistical standard deviations of the last digits for the fitted parameters, and not the much larger correlated and possibly systematic errors, especially for K_0'.

	V_0 (cm^3 mol^{-1})	K_0 (GPa)	K_0'
KCl ($cP2$)	32.4 (4)[a]	22.2 (23)[a]	4.93 (8)[a]
KBr ($cP2$)	37.9 (5)	17.0 (16)	5.38 (8)
KI ($cP2$)	49.0 (6)	10.1 (7)	5.77 (8)
RbCl ($cP2$)	36.7 (3)	18.2 (16)	5.37 (8)
RbBr ($cP2$)	42.2 (6)	14.8 (16)	5.67 (8)
RbI ($cP2$)	52.8 (8)	10.1 (10)	5.93 (8)
CsCl ($cP2$)	42.185[b]	17.0 (18)	5.58 (9)
CsBr ($cP2$)	47.722[b]	14.8 (12)	5.80 (7)
CsI ($cP2$)	57.397	11.89 (5)[c]	5.93 (8)[c]

because all of the intense lines from the sample corresponded to the same $\Gamma(hkl) = 0.25$ in this evaluation. However, since the elastic coefficients for both sample and marker lead to similar corrections when NaCl is used as the marker, and to opposing corrections with Au and Cu as the marker, the differences between the measurements with these different groups of markers allow an estimate to be made of possible corrections from these deviatoric stresses. Au and Cu showed thereby only larger scattering with respect to the fitted EOS, and, at the most, a systematic deviation with respect to the NaCl data of 2% at 30 GPa, which could be due to the deviatoric stresses. These effects together reduce the total accuracy in

the lattice parameter determination for these cubic substances to 0.2%, which corresponds to $\sigma_p = 5\%$ of the measurements with the NaCl marker.

5. Results

The data from the present experiments are shown in figures 3–5. Experiments with different pressure sensors are denoted by different symbols, and the solid lines represent the fitted H11-EOS forms. Most of the experiments were performed with increasing pressures (full symbols), but some of the data were also taken with decreasing pressure (open symbols). No systematic deviations are observed in these pressure cycles.

For the potassium and rubidium halides, both K_0 and V_0 were used as free parameters in the H11 fits, but for the caesium halides K_0 was the only fitting parameter. Table 2 gives the results of these fits.

A glance at figures 3–5 shows that the scatter of the data obtained with the ruby-luminescence technique or the metal markers is somewhat larger than for the experiments using NaCl as the marker substance. Quantitatively, the standard deviations are $\sigma_p = 5\%$ for the experiments with NaCl, $\sigma_p = 10\%$ for the Au and Cu markers, and $\sigma_p = 11\%$ for the experiments with the ruby sensors. This larger uncertainty in the experiments with ruby, Au, and Cu was taken into account by means of corresponding weights in the fits of the EOS form to the data.

The higher precision of the measurements with NaCl as the pressure marker is not completely unexpected. First of all, the ruby splinters can only monitor the pressure at one special location in the sample space, which will not represent the average pressure of the measured sample, if pressure gradients are present. This problem is avoided with the pressure markers Au and Cu, if these marker substances are intimately mixed with the sample. However, the larger stiffness of the metal markers, in comparison with NaCl and the other salts used in the measurements, leads first to a lower precision in the pressure measurements, due to the smaller changes in the lattice parameters, and, in addition, to larger contributions from deviatoric stresses, due to the additional elastic–plastic deformation around the stiffer particles.

6. Comparison with literature data

To help in visualizing the uncertainties in high-pressure x-ray data, various 'linearization schemes' have been introduced [5, 6]. The generalized stress [6]

$$\eta = \ln\left(\frac{p}{p_{FG0}}\right) - \ln(1 - X) + 5\ln X \tag{7}$$

gives for ambient pressure ($X = 1$)

$$\eta_0 = \ln\left(\frac{3K_0}{p_{FG0}}\right) = -c_0. \tag{8}$$

Figures 6–8 show that the present data and also the additional data from the literature fit to the linear interpolation between $\eta(X = 0) = 0$ and $\eta(X = 1) = \eta_0$ which corresponds to the H11 form (1). The NaCl results are represented by full circles, and the Au, Cu, and ruby data by open circles, respectively. The solid straight lines represent the H11-EOS forms. References to the literature data are given in the figures.

Figure 6 illustrates these η–X plots for the potassium halides. The present results for KBr and KI show first of all close agreement with the volumetric data [28, 29] at low

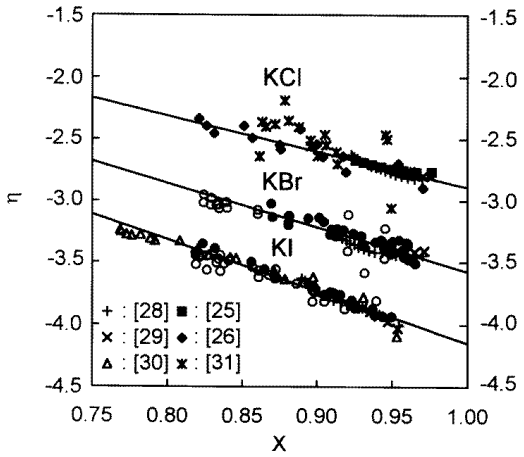

Figure 6. An η–X plot (see the text) of the present data for KBr and KI (solid circles: experiments with the NaCl marker; open circles: Au, Cu, and ruby experiments) for comparison with the literature data (references are given in the figure). The solid lines represent the H11 form.

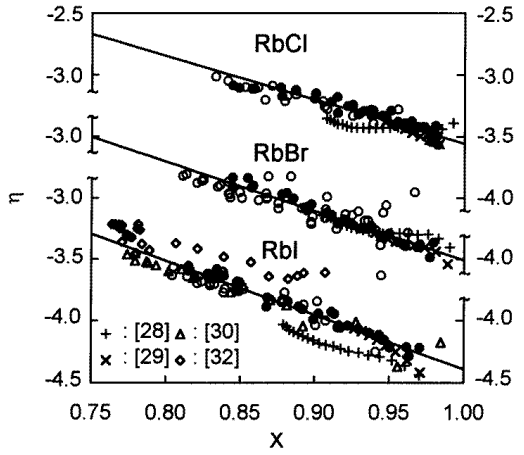

Figure 7. An η–X plot (see the text) of the present data for RbCl, RbBr, and RbI (solid circles: experiments with the NaCl marker; open circles: Au, Cu, and ruby experiments) for comparison with the literature data (references are given in the figure). The solid lines represent the H11 form.

pressures, and also with the previous x-ray data for KI extending even to higher pressures [30]. It can be noted that nearly all of the data are in good agreement with the respective H11-EOS, except the earliest x-ray data for KCl [31], which also show larger scatter.

The data for the rubidium halides are shown in figure 7. Some distinct differences between the earlier results of volumetric [28, 29] and x-ray [30, 32] measurements on RbI can be noticed, and the present data fit very closely to the results of reference [30]. For RbCl the volumetric data [28, 29] show similar systematic deviations with respect to the present results to those in the case of RbI, while the agreement in the case of RbBr is quite good for all of the data.

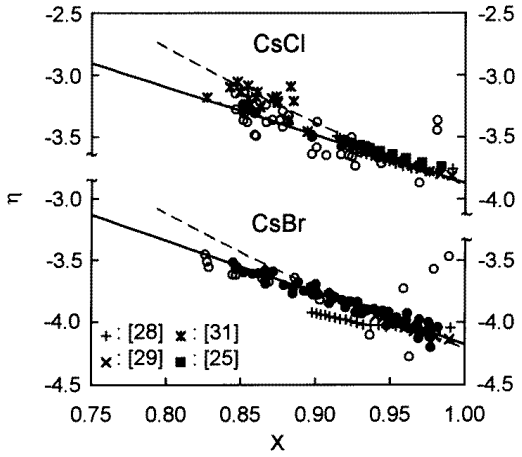

Figure 8. An η–X plot (see the text) of the present data for CsCl and CsBr (solid circles: experiments with the NaCl marker; open circles: Au and ruby experiments) for comparison with the literature data (references to the data points are given in the figure). The solid lines represent the H11 form, the dashed lines reproduce the proposed Birch EOS based on ultrasonic data [8]. Decker's semi-empirical EOS for CsCl [16] coincides with the H11 curve.

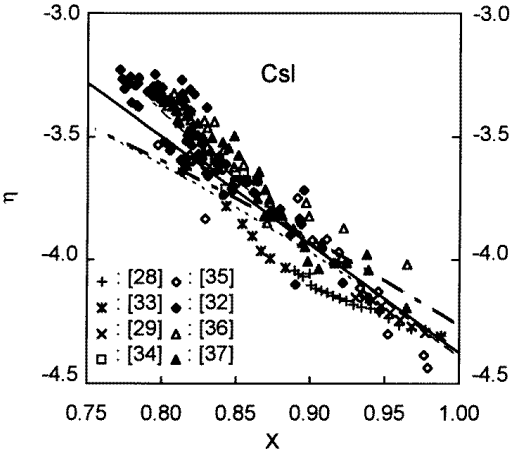

Figure 9. An η–X plot of the literature data for CsI (references for the data points are given in the figure). The solid line represents the H11 form based on the ultrasonic value for K_0 [8]. The dashed line (hardly discernible) reproduces the Birch EOS based on ultrasonic data [8], the dotted line illustrates the result of APW calculations [39], and the chain line represents the most recent x-ray data fitted to the 'universal EOS' form [38].

The caesium halides already exhibit the $cP2$-structure at ambient conditions, and a third-order Birch EOS form was proposed, together with the values for K_0, K_0', and K_0'' from ultrasonic measurements [8]. These EOS forms are shown as dashed lines in figure 8, together with all of the experimental data.

Decker has determined also an EOS for CsCl in the same way as for his well-known EOS of NaCl [16]. This EOS form coincides with the H11 form based on the present data, and is therefore not visible in figure 8.

7. Discussion

The present study shows first of all that the EOS data for all of the alkali halides studied so far in their $cP2$-phase are perfectly represented by the first-order H11 form within the experimental precision of $\sigma_p = 5\%$ with respect of the standard EOS of NaCl [16], and also within the somewhat larger standard deviations of $\sigma_p = 10\%$ for the metal markers Au and Cu, or $\sigma_p = 11\%$ with respect to the ruby scale.

At first this observation was made for CsCl and CsBr, which already exhibit the $cP2$-structure at ambient conditions, with accurate information on V_0- and K_0-values from x-ray and ultrasonic measurements, respectively, leaving no free parameter for the fits, since K_0' is related in the form H11 directly to V_0 and K_0 as given by equations (3) to (5). These results motivated the use of the form H11 also for the high-pressure $cP2$-phases, where H11 reduces the number of free parameters to just two, namely V_0 and K_0 with the correlated value of K_0'. These fits resulted in more narrowly bounded and more systematically varying values for these parameters than in any previous study.

Significant deviations of the H11 form from literature data [28, 29, 32–39] were only noticed for CsI at pressures above 15 GPa, corresponding to $X = 0.876$ in figure 9, where CsI undergoes a distortive phase transition to an orthorhombic structure. In this case the revised indexing [38] of the earlier data leads also to a more reasonable agreement with the extrapolated H11 form, from the point of view that it gives a minor softening (lower values) in the distorted high-pressure phase compared to an unreasonable hardening (higher values) according to the initial indexing scheme.

In any case, the present determinations of EOS data for RbCl and RbBr over an extended range, under pressures up to 40 and 50 GPa, respectively, are of special interest also for other high-pressure x-ray diffraction measurements using the EDXD method, since these two substances can be considered as very reasonable alternatives to the caesium halides for pressure determinations, offering the advantage, that (i) no fluorescence lines disturb the interesting energy range between 20 and 80 keV, (ii) similar softness to that for the caesium halides guarantees the same resolutions in pressure determinations at moderate pressures, and (iii) higher resolution is obtained in the higher-pressure region, where the caesium halides show their distortive transitions. The low shear strength and the low-pressure phase transitions in RbCl and RbBr at around 0.5 GPa guarantee thereby also lower deviatoric stresses at higher pressures than most of the other calibrants, since the deviatoric stresses due to the initial compaction of these samples are largely relaxed in these transitions, which, most probably, lowers the total level of deviatoric stresses also at higher pressures.

References

[1] Johannsen P G, Reiß G, Bohle U, Magiera J, Müller R, Spiekermann H and Holzapfel W B 1997 *Phys. Rev.* B **55** 6865

[2] Here in brackets, and later on in the text, Pearson's nomenclature is used; see, e.g., *IUPAC: Nomenclature of Inorganic Chemistry* 1990 ed G J Leigh (Oxford: Blackwell Scientific)

[3] Holzapfel W B 1996 *High Pressure Science and Technology* ed W A Trzeciakowski (Singapore: World Scientific) p 69

[4] Johannsen P G 1997 *Phys. Rev.* B **55** 6856

[5] Birch F 1978 *J. Geophys. Res.* **83** 1257
Heinz D L and Jeanloz R 1984 *J. Appl. Phys.* **55** 885
Vinet P, Ferrante J, Smith J R and Rose J H 1986 *J. Phys. C: Solid State Phys.* **19** L467
Smith G S 1989 *Phys. Lett.* **A140** 431

[6] Holzapfel W B 1991 *Europhys. Lett.* **16** 67
Holzapfel W B 1991 *High Pressure Res.* **7** 290

[7] Roberts R W and Smith C S 1970 *J. Phys. Chem. Solids* **31** 619
Roberts R W and Smith C S 1970 *J. Phys. Chem. Solids* **31** 2387
McLean K O and Smith C S 1972 *J. Phys. Chem. Solids* **33** 279
Smith C S and Cain L S 1975 *J. Phys. Chem. Solids* **36** 205
[8] Barsch G R and Chang Z P 1971 *Accurate Characterization of the High-Pressure Environment* NBS Special Publication 326, ed E C Lloyd (Washington, DC: US Government Printing Office) p 173
[9] Born M and Huang K 1954 *Dynamical Theory of Crystal Lattices* (Oxford: Clarendon)
[10] Tosi M P 1964 *Solid State Physics* vol 16, ed F Seitz and D Turnbull (New York: Academic) p 1
[11] The values are based on the interionic distances given in reference [7].
[12] Johannsen P G 1997 to be published
[13] Syassen K and Holzapfel W B 1975 *Solid State Commun.* **16** 533
[14] Holzapfel W B 1978 *High Pressure Chemistry* ed H Kelm (Dordrecht: Reidel) p 177
[15] Suprapur (Merck).
[16] Decker L D 1971 *J. Appl. Phys.* **42** 3239
[17] Mao H K, Bell P M, Shaner J W and Steinberg D J 1978 *J. Appl. Phys.* **49** 3276
[18] Bell P M, Xu J A and Mao H K 1986 *Shock Waves in Condensed Matter* ed Y M Gupta (New York: Plenum)
[19] White mineral oil (Merck).
[20] Foreman R A, Piermarini G J, Barnett J D and Block S 1972 *Science* **176** 284
[21] Großhans W A, Düsing E F and Holzapfel W B 1984 *High Temp.–High Pressures* **16** 539
[22] Otto J W 1994 *HASYLAB, DESY, Hamburg, Annual Report 1993* p 931
[23] Singh A K and Kennedy G C 1974 *J. Appl. Phys.* **45** 4686
Singh A K and Balasingh C 1977 *J. Appl. Phys.* **48** 5338
[24] Singh A K 1993 J. *Appl. Phys.* **73** 4278
[25] Yagi T 1978 *J. Phys. Chem. Solids* **39** 563
[26] Campbell A J and Heinz D L 1991 *J. Phys. Chem. Solids* **52** 495
[27] *Powder Diffraction File* 1967 vol 6, ed L G Berry (Swarthmore, PA: Joint Committee on Powder Diffraction Standards) p 44
[28] Kennedy G C and Keeler R N 1972 *American Institute of Physics Handbook* 3rd edn (New York: McGraw-Hill)
[29] Vaidya S N and Kennedy G C 1971 *J. Phys. Chem. Solids* **32** 951
[30] Asaumi K, Suzuki T and Mori T 1983 *Phys. Rev.* B **28** 3529
[31] Drickamer H G, Lynch R W, Clendenen R L and Perez-Albuerne E A 1966 *Solid State Physics* vol 19 (New York: Academic) p 135
[32] Vohra Y K, Brister K E, Weir S T, Duclos S J and Ruoff A L 1986 *Science* **231** 1136
[33] Hammond D E 1974 *Advances in High Pressure Research* vol 4, ed R H Wentorf (New York: Academic) p 161
[34] Ruoff A L, Vohra Y K, Brister K E and Weir S 1986 *Physica* B **139+140** 209
[35] Zisman A N, Aleksandrov I V and Stishov S M 1985 *Phys. Rev.* B **32** 484
[36] Knittle E and Jeanloz R 1984 *Science* **223** 53
Knittle E and Jeanloz R 1985 *J. Phys. Chem. Solids* **46** 1179
[37] Asaumi K 1984 *Phys. Rev.* B **29** 1118
[38] Mao H K, Wu Y, Hemley R J, Chen L C, Shu J F, Finger L W and Cox D E 1990 *Phys. Rev. Lett.* **64** 1749
[39] Aidun J, Bukowinski M S T and Ross M 1984 *Phys. Rev.* B **29** 2611